



## Effects of nitrogen metabolism on growth and aflatoxin biosynthesis in *Aspergillus flavus*



Bin Wang<sup>a,1</sup>, Xiaoyun Han<sup>a,1</sup>, Youhuang Bai<sup>a,1</sup>, Zhenguo Lin<sup>b</sup>, Mengguang Qiu<sup>a</sup>, Xinyi Nie<sup>a</sup>, Sen Wang<sup>a</sup>, Feng Zhang<sup>a</sup>, Zhenhong Zhuang<sup>a</sup>, Jun Yuan<sup>a</sup>, Shihua Wang<sup>a,\*</sup>

<sup>a</sup> Key Laboratory of Pathogenic Fungi and Mycotoxins of Fujian Province, Key Laboratory of Biopesticide and Chemical Biology of Education Ministry, School of Life Sciences, Fujian Agriculture and Forestry University, Fuzhou 350002, China

<sup>b</sup> Department of Biology, Saint Louis University, St. Louis, MO 63103, United States

### HIGHLIGHTS

- Glutamine was the optimal nitrogen source for AFB1 production in *A. flavus*.
- 4 mM Gln was a threshold for AFB1 production and *A. flavus* growth.
- Rapamycin suppressed AFs production, fungal growth and conidiation.

### ARTICLE INFO

#### Article history:

Received 5 May 2016

Received in revised form

14 November 2016

Accepted 16 November 2016

Available online 21 November 2016

#### Keywords:

*Aspergillus flavus*

Aflatoxins

Nitrogen sources

Glutamine

RNA-seq

### ABSTRACT

Aflatoxins (AFs), produced mainly by *Aspergillus flavus* and *Aspergillus parasiticus*, are strongly toxic and carcinogenic. Here, we showed that glutamine is the optimal nitrogen source for AF-production in *A. flavus* grown in Czapek Dox medium. Additionally, 4 mM glutamine was the threshold for high production of aflatoxin B<sub>1</sub>. However, no significant impact of glutamine synthetase inhibitor was detected for on AF biosynthesis. In contrast, rapamycin could significantly suppress the glutamine inducing effect on AFs production, simultaneously inhibiting the fungal growth and conidiation. To identify the genes and regulatory networks involved in AFs biosynthesis, especially concerning the nitrogen source metabolism pathway and the target of rapamycin (TOR) signaling pathway, we obtained transcriptomes for *A. flavus* under treatment of three nitrogen sources by RNA-sequencing. We identified 1429 differentially expressed genes. Through GO and KEGG pathway analyses, the relationship between nitrogen metabolism and AFs biosynthesis was revealed, and the effects of TOR inhibitor were confirmed. Additionally, the quantitative real-time PCR results verified the credibility and reliability of the RNA-seq data, and were consistent with the other experimental results. Our research laid the foundation for a primary study on the involvement of the nitrogen regulatory network and TOR signaling pathway in AF biosynthesis.

© 2016 Elsevier B.V. All rights reserved.

### 1. Introduction

*Aspergillus flavus* is a notorious saprobe and opportunistic plant pathogen infecting and contaminating a wide range of economically important grains worldwide [1–5]. Aflatoxins (AFs) are mainly produced by *A. flavus* and *Aspergillus parasiticus*, and pre- and postharvest infestations of grains with the secondary metabolites (SMs) of AFs [Aflatoxin B<sub>1</sub> (AFB<sub>1</sub>), B<sub>2</sub>, G<sub>1</sub> and G<sub>2</sub>] are common [6].

Animals and humans are also the victims of aflatoxicosis, liver cancer, and even death, through the consumption of contaminated feed and food [7,8].

The molecular mechanisms of AF production have attracted global attention [9]. An extensive effort to elucidate the process of AF biosynthesis has recently revealed that more than 30 genes were involved in AF formation in *A. flavus* [5,10]. Moreover, water, temperature, nutrients, and other physicochemical factors were found to have a remarkable influence on AF biosynthesis [8,11,12]. However, the way in which AF biosynthesis is affected by environmental influences remains an enigma [5,13–15].

Nitrogen is an essential nutrient for fungal growth, and fungi can use a wide variety of compounds as nitrogen sources [16], including ammonium and glutamine, which are preferentially used over com-

\* Corresponding author.

E-mail addresses: [15980692732@163.com](mailto:15980692732@163.com) (X. Han), [wshyy1@sina.com](mailto:wshyy1@sina.com) (S. Wang).

<sup>1</sup> These authors contributed to this work equally.

plex sources [17]. The preferential use of these readily assimilated compounds was accomplished by nitrogen catabolite repression, which is primarily regulated at the transcriptional level [16]. In *A. parasiticus*, the quality and quantity of the nitrogen source used in the growth medium may have different effects on AF production [6,18,19]. For instance, asparagine-, aspartate-, alanine-, proline-, glutamate-, glutamine- and ammonium-containing media were shown to support AF production, while nitrate- and nitrite-containing media did not [5,18,19]. For the substrate-specific gene activation, additional pathway-specific transcription factors were involved, mediating the induction of a gene set in response to a specific inducer [20–22]. It was proposed that nitrogen sources act as metabolic switches to trigger the expression of infection-related genes in plant pathogenic fungi [23].

It has been widely recognized that a central regulator of cell growth in response to nutrients (nitrogen sources) is the protein kinase Target Of Rapamycin (TOR), which is evolutionarily conserved in all eukaryotic life forms [23–25]. In *Saccharomyces cerevisiae*, the inhibition of TOR by rapamycin caused cell cycle arrest and nutrient stress responses. Furthermore, both nitrogen starvation and rapamycin processing resulted in the rapid dephosphorylation and nuclear accumulation of Gln3, a global regulator controlling the expression of a large number of genes involved in nitrogen metabolism [25,26]. A homolog of Gln3 in *Aspergillus*, AreA, showed similar phenotypes [27–29]. However, little is known about how TOR senses nitrogen signals and transduced the signals to transcription factors to elicit responses [30]. Therefore, further studies should be performed.

Our previous findings showed that compared with  $\text{NaNO}_3$ , glutamine is a preferred nitrogen source and could promote AFB<sub>1</sub> production. In addition, rapamycin treatment suppressed the glutamine effect on AFs biosynthesis, restrained the fungal growth and conidiation. This study aimed to explore possible crosstalk between nitrogen signaling and the TOR cascade in the regulation of AF biosynthesis in *A. flavus* [31–33]. To determine the potential networks of nitrogen signaling in the regulation of AF biosynthesis and the TOR pathway, we used high-throughput RNA sequencing (RNA-seq), which revealed abundant numbers of differentially expressed genes (DEGs) in three groups:  $\text{NaNO}_3$  (N), glutamine (G) and glutamine plus rapamycin (R) treatments. The transcriptome sequencing analysis revealed that the DEGs were mainly involved in nitrogen metabolism, secondary metabolite biosynthesis, and AF biosynthesis pathways. Thus, our research played a crucial role in exploring the regulatory networks of AF production, nitrogen metabolism, and TOR signaling, and laid a foundation for controlling the harm caused by mycotoxins.

## 2. Experimental procedures

### 2.1. Fungal isolate and culture conditions

The *A. flavus* wild-type NRRL3357, kindly provided by Prof. Zhumei He (Sun Yat-sen University, Guangzhou, China), was used in all of the experiments. All of the strains were maintained as glycerol stocks and grown on solid Czapek Dox (CD) medium at 28 °C in the dark. Detailed composition of 1 L CD medium is as follows: 30 g of sucrose, 3 g of  $\text{NaNO}_3$ , 1 g of  $\text{K}_2\text{HPO}_4$ , 0.5 g of KCl, 0.5 g of  $\text{MgSO}_4 \cdot 7\text{H}_2\text{O}$ , 0.01 g of  $\text{FeSO}_4$ , 20 g of agar. Replaceable nitrogen sources, including ammonium chloride ( $\text{NH}_4\text{Cl}$ ), ammonium sulfate [ $(\text{NH}_4)_2\text{SO}_4$ ], ammonium nitrate ( $\text{NH}_4\text{NO}_3$ ), urea, asparagine, aspartate, glutamate, Gln, alanine, proline, and tyrosine, and rapamycin (Sigma-Aldrich, St Louis, USA) were added to the CD medium to the desired final concentrations after autoclaving. All of the experiments included three replicate plates and were performed at least twice.

### 2.2. Growth on different nitrogen sources

The different nitrogen source-containing media were inoculated in the middle with 2.5  $\mu\text{L}$  of a  $4 \times 10^5$  conidia/mL suspension to assess growth rates [12], and the growth status was observed and photographed daily.

### 2.3. AFs extractions and analyses

To analyze AF production, AFs were extracted from 500  $\mu\text{L}$  extract obtained from *A. flavus* cultures with an equal volume of chloroform. The chloroform layer transferred to a new 1.5 mL tube and was evaporated to dryness at 70 °C. Next, thin layer chromatography (TLC), consisting of acetone:chloroform (1:9, v/v) solvent system was used to analyze AF biosynthesis, and the results were observed under ultraviolet light at 365 nm.

### 2.4. Conidial observation

The conidial amount produced was determined by removing three plugs (1.5 cm  $\times$  1.5 cm) from each colony. Conidial suspensions were viewed using a Leica inverted microscope (Leica Microsystems). The conidia from each plug were suspended in a solution of 0.01% Tween 20 and counted in an hemocytometer.

### 2.5. Impact of Gln concentrations on AF biosynthesis

To quantify AF production under 1–6 mM Gln, a MYCOTOX™ reversed-phase ( $\text{C}_{18}$  column, 4.6  $\times$  250 mm) high-performance liquid chromatography 1525 (HPLC, Waters, Milford, MA, USA) was used. The AF extract was filtered (0.22  $\mu\text{m}$ ), detected and analyzed. The column was equilibrated in the mobile phase (56:22:22, water:methanol:acetonitrile) at 42 °C, and 10  $\mu\text{L}$  was injected and run isocratically for 15 min with 100% mobile phase at a flow rate of 1.0 mL/min. A fluorescent detector with an excitation wavelength of 365 nm and an emission wavelength of 430 nm was used to detect AFs [34]. The individual stock solutions of AFB<sub>1</sub> and AFB<sub>2</sub> (100 mg/mL) were purchased from Sigma and stored at –20 °C. Ten working standard solutions of AFB<sub>1</sub> and AFB<sub>2</sub> (10, 20, 30, 40, 50, 60, 70, 80, 90 and 100 mg/mL) were prepared by diluting and mixing each stock standard solution with methanol. Calibration curves were constructed using working standard solutions by plotting the peak area.

### 2.6. RNA extraction and quality testing

Three comparison colonies,  $\text{NaNO}_3$  (N), glutamine (G) and glutamine plus rapamycin (R), were vegetatively grown on solid Czapek Dox medium at 28 °C for 30 h to obtain enough biomass. Total RNA was extracted from 100 mg of fungal mycelia using TRIzol reagent (Invitrogen, Carlsbad, CA) according to the manufacturer's instructions. The purity of the total RNA was detected using a Nano-Drop 2000 spectrophotometer (Thermo Fisher Scientific, Inc.), and the integrity of the RNA samples was assessed using an Agilent 2100 Bioanalyzer (Agilent Technologies, Inc.). The purified RNA was dissolved in RNase-free water and stored at –80 °C.

### 2.7. RNA-seq library construction and sequencing

The construction of RNA-seq library was performed using the NEBNext Ultra RNA Library Prep Kit for Illumina (New England Biolabs, Inc.) following the manufacturer's instructions. Briefly, for total RNA, mRNA isolation, fragmentation and priming were performed using the NEBNext Poly(A) mRNA Magnetic Isolation Module (NEB #E7490). Double-stranded cDNAs were synthesized

using fragmented-primed mRNA, Murine RNase inhibitor and ProScript II reverse transcriptase, followed by the second-strand reaction buffer (10×) and second-strand synthesis enzyme mix. They were purified with 1.8× Agencourt AMPure XP beads followed by the end repair/dA-tailing of the cDNA library. Then, NEBNext adapter oligonucleotides were ligated to cDNA fragments, and the AMPure XP beads system (Beckman Coulter, Beverly, USA) was used to select larger sized fragments (>200 nt). Suitable cDNA fragments were selected as templates for PCR amplification using the NEB universal PCR primer and index primer. Products were purified with the AMPure XP bead system and quantified using a Bioanalyzer (Agilent high sensitivity chip). Finally, RNA-seq libraries were sequenced using an Illumina HiSeq 2500 at Fujian Agriculture and Forestry University sequencing center (Fuzhou, China).

### 2.8. Transcriptome annotation and analysis

The genome and annotation data of *A. flavus* were downloaded from the Ensembl Fungi database. Illumina adapters were trimmed from the raw reads, which were further filtered with recommended parameters (-l 35 -q 30 -w 4 -x 10) using the “fastq-mcf” tool from the ea-utils package ([code.google.com/p/ea-utils/wiki/FastqMcf](http://code.google.com/p/ea-utils/wiki/FastqMcf)). The filtered reads were mapped to the *A. flavus* genome using Tophat v 2.0.12. Cufflinks [35] was used to assemble the transcripts and to calculate gene expression levels in both the “fragments per kilobase of exon model per million mapped reads” (FPKM) and “raw counts” modes. A list of differential expression genes (DEGs) was identified using the R packages’ EdgeR [36].

Gene Ontology (GO) annotation file of *A. flavus* genes was downloaded from the UniProt. GO enrichment analysis of DEGs was conducted in the “BiNGO” and “Enrichment Map” plugins of the Cytoscape software [37]. Enrichment analysis of DEGs in the Kyoto Encyclopedia of Gene and Genomes (KEGG) biological pathway was conducted on the FungiFun2 website with default parameters.

### 2.9. Quantitative real-time RT-PCR assays

Quantitative real-time RT-PCR (qRT-PCR) analyses were performed with independent samples from N, G and R at the same developmental stages as those used for the RNA-seq analysis. cDNAs were reversely transcribed using the RevertAid First Strand cDNA Synthesis Kit (Thermo Scientific, Inc.), and qRT-PCR analyses were performed on a PIKO REAL Real-Time PCR System (Thermo Scientific, Inc.) using TransStart Top Green qPCR SuperMix (TransGen Biotech, Beijing, China). The qRT-PCR conditions were as follows: 95 °C for 7 min and 40 cycles of 95 °C for 5 s and 60 °C for 30 s. The *A. flavus*  $\beta$ -tubulin gene was used as an internal control to normalize the expression data. The relative expression of genes was calculated using the  $2^{-\Delta\Delta Ct}$  method, and the standard deviation was calculated from three biological replicates [38]. The gene-specific primers are listed in **Table S1**.

### 2.10. Accession numbers

All RNA-seq data have been submitted to the NCBI Sequence Read Archive (SRA) (<http://www.ncbi.nlm.nih.gov/sra/>) under the accession number SRP064723 (<https://www.ncbi.nlm.nih.gov/sra/?term=SRP064723>). The accession numbers of RNA-seq datasets used in this study are listed in **Table S1** and **Table S2**.

## 3. Results

### 3.1. AF production in response to various nitrogen sources

A previous study showed that *A. flavus* strains germinated on the CD medium, but produced limited amounts of AFs, which

was likely related to the use of the NaNO<sub>3</sub> nitrogen source in the CD medium [5,18,19]. Thus, we investigated the effects of other nitrogen sources on AF production and growth. There was little difference among the growth states (Fig. 1A), which corroborated the results of Fernandez, who found that there were only slight differences in mycelial growth in the presence of a sole repressing carbon source, regardless of the nitrogen sources [39]. Mycelial growth on a medium containing NH<sub>4</sub>Cl and (NH<sub>4</sub>)<sub>2</sub>SO<sub>4</sub> did not increase after the sixth day. Conversely, the growth rate on the NH<sub>4</sub>NO<sub>3</sub> medium was different from the rates on NH<sub>4</sub>Cl- and (NH<sub>4</sub>)<sub>2</sub>SO<sub>4</sub>-containing media—despite each having ammonium—but was the same as with other nitrogen sources (data not shown). The medium containing tyrosine appeared opaque owing to its low solubility, but the mycelial growth remained unaffected (Fig. 1A). Quantitative analysis results of AF production showed that all of the selected replaceable nitrogen sources supported AFB<sub>1</sub> formation, and ammonia and urea were able to promote a small amount of AFB<sub>1</sub>, with NH<sub>4</sub>NO<sub>3</sub> accumulating the most. Compared with ammonia and urea, amino acids could induce relatively higher quantities of AFB<sub>1</sub> biosynthesis, and the maximum level of Gln accumulated (Fig. 1B and C). Thus, different nitrogen sources had little effect on mycelial growth, but affected AF biosynthesis, and Gln could promote the highest AF production in *A. flavus*.

### 3.2. Effects of Gln concentrations on AF production and growth

Previous research showed that the concentrations of nitrogen resources could affect AF biosynthesis in *A. flavus* and *A. parasiticus* [5], but it was not clear whether Gln concentrations affected AF biosynthesis. Our previous results showed that there was little difference in AF production among Gln concentrations of 6, 60, 90 and 120 mM (Fig. S1). Therefore, we carried out the experiments below. Apparently, AFB<sub>1</sub> production increased under 1–4 mM Gln, but no longer increased when the Gln concentration was at 4–6 mM (Fig. 2B–D). Thus, we concluded that 4 mM Gln was the low concentration threshold for AFB<sub>1</sub> production. In addition, other SMS increased at 4–6 mM Gln (marked by arrows in Fig. 2C). These results indicated that Gln metabolism might be involved in AF biosynthesis directly or regulate the expression of genes in the AF biosynthesis pathway. Additionally, Gln concentrations also had certain influences on the growth phenotype. The growth of *A. flavus* showed the nitrogen source-limited phenotype at 1–3 mM Gln concentrations, but *A. flavus* growth had a fluffy-like morphology at 4–6 mM Gln (Fig. 2A), which might be a response to the limited nitrogen source under undesirable circumstances. In short, these results indicated that 4 mM Gln was the nitrogen source limiting threshold for the AFB<sub>1</sub> production and *A. flavus* growth.

### 3.3. Effects of Gln synthetase inhibitor treatment on AF production and growth

From the results above, we inferred that Gln might be the nitrogen source signal for AF formation, and other nitrogen sources could be transformed into Gln and then regulate AF biosynthesis. Thus, the Gln synthetase (GS) inhibitor methionine sulfoximine (MSX) was used to deplete the intracellular Gln and then the influences of nitrogen sources on AF production were observed. Unexpectedly, we found that the MSX processing seemed to have little impact on AF production (Fig. 3B and C). Studies on the possible regulatory mechanism of MSX on AF biosynthesis need to be continued. However, the hyphae presented a fluffy-like growth phenotype after MSX treatment (Fig. 3A). These results suggested that the regulatory mechanisms of the MSX treatment on AF biosynthesis and growth were different, indicating that there were sophisticated regulatory mechanisms for AF biosynthesis and *A. flavus* growth.

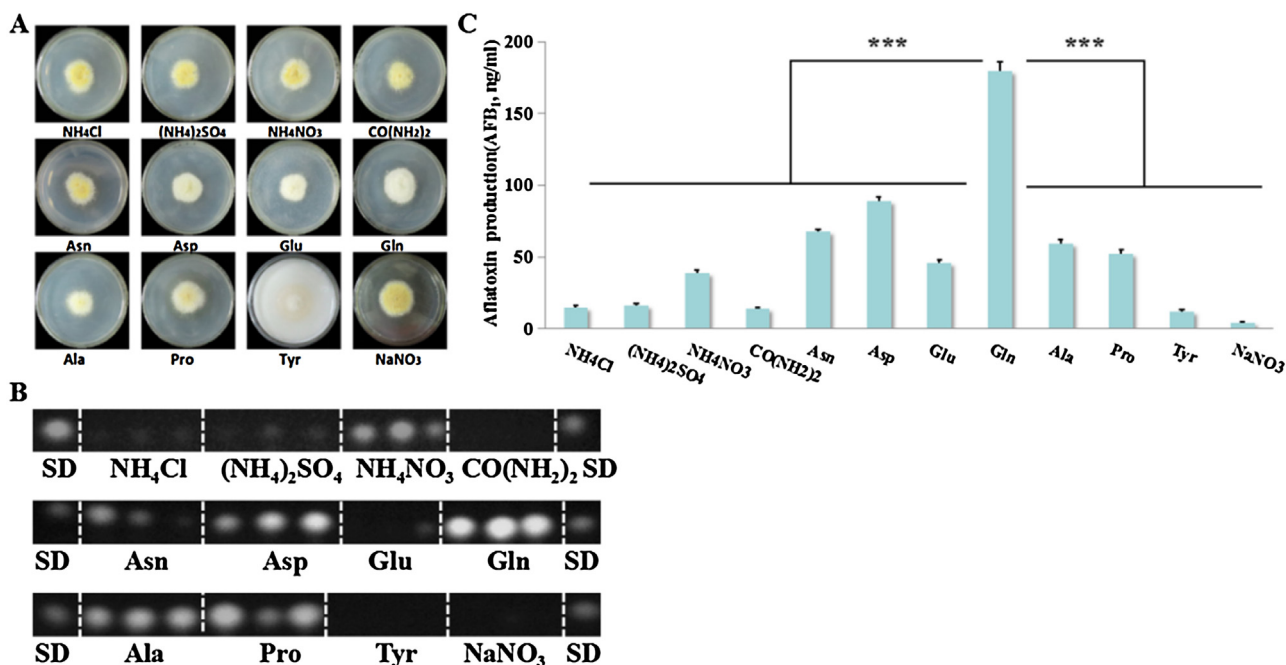


**Fig. 1.** Gln induces the maximal AFB<sub>1</sub> biosynthesis in *A. flavus*. A. Morphological characterization of five-day-old strains cultured in different nitrogen sources (see Experimental procedures). B. TLC results of metabolite extracts to determine AFs production (AFB<sub>1</sub>) from *A. flavus* grown on different nitrogen sources for seven days in the dark. SD means standard AFB<sub>1</sub>. C. Quantitative analysis of AFB<sub>1</sub> production by JD image analysis system software. Bars represent standard deviation from three independent experiments with three replicates each, \*\*\*Significant at  $P < 0.001$  as determined by Student's *t*-test.

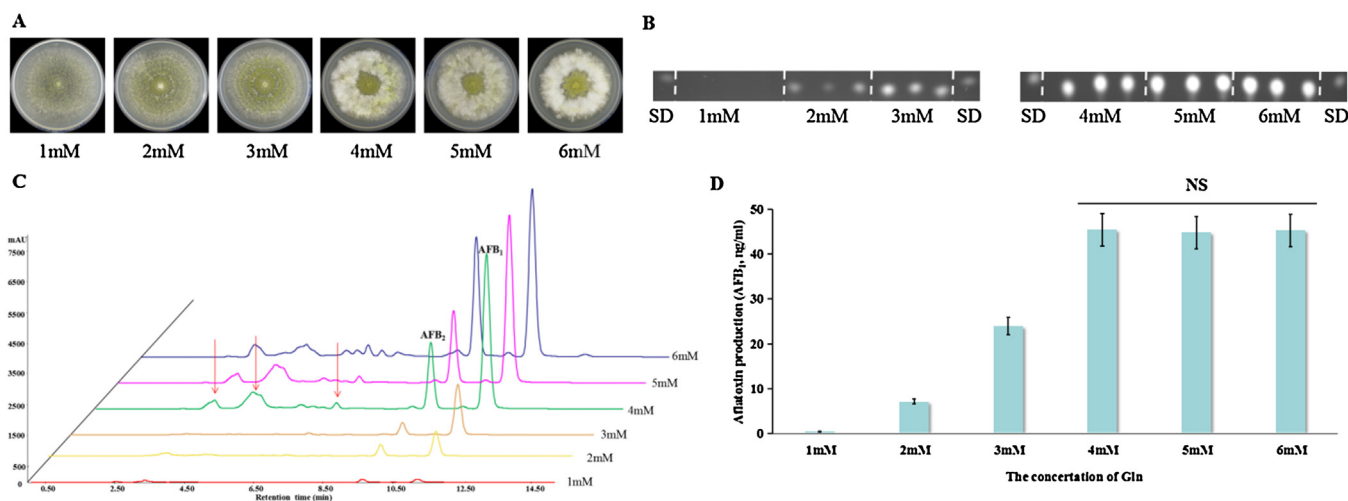


**Fig. 2.** Different concentrations of Gln affected aflatoxin biosynthesis. A. Morphological characterizations of four-day-old colonies cultured on media containing 1–6 mM Gln, respectively. B. TLC results of AFs produced by seven-day-old colonies of *A. flavus* grown on 1–6 mM Gln, respectively. SD is a standard product of AFB<sub>1</sub>. C. Chromatogram of AFs and other secondary metabolites. D. Quantitative results of AFB<sub>1</sub> by HPLC. Bars represent standard deviation from two independent experiments with four replicates each, and NS denotes no significant differences at  $P > 0.05$  as determined by Student's *t*-test.

### 3.4. Effects of rapamycin on growth, conidia and AF biosynthesis

*A. flavus* that germinated on a CD medium containing NaNO<sub>3</sub> produced no AFs, and Gln supported the highest AF production. Previous studies reported that nitrogen sources could regulate SMs biosynthesis through the TOR signaling pathway in fungi [31,32]. To investigate the possible relationships among nitrogen metabolism, AF biosynthesis and the TOR signaling pathway, *A. flavus* strains were treated with the TOR inhibitor rapamycin and the phenotypic characteristics were observed. Apparently, the rapamycin treatment restrained growth, and conidia and AF production (Fig. 4A–D), which are related to the blockage of the TOR signaling cascade [30,40]. This suggested a certain relationship between the nitro-

gen regulatory network and the TOR kinase pathway involved in AF production: (1) nitrate repressed AF formation but Gln promoted it, and (2) AF biosynthesis was inhibited when the TOR kinase pathway was suppressed. However, the molecular mechanisms of the triadic relationship remain poorly understood.

### 3.5. Gene expression comparisons among RNA-seq groups

To investigate the potential gene expression networks of the nitrogen response and TOR kinase pathways in the regulation of AF biosynthesis, *A. flavus* vegetatively grown on three different nitrogen sources NaNO<sub>3</sub>(N), glutamine (G) and glutamine plus rapamycin (R), we sampled and analyzed using RNA-seq. About

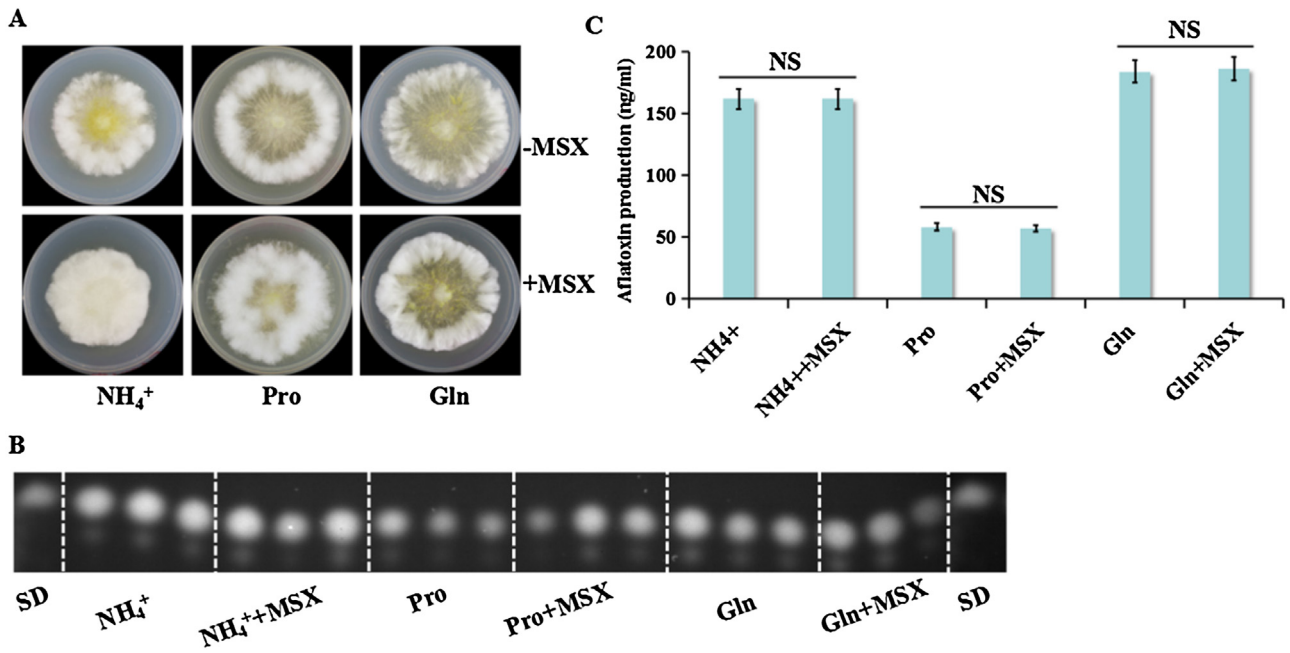


**Fig. 3.** The effect of MSX treatment on the growth and AFs-production in *A. flavus*. A. The effect of MSX treatment on the growth of *A. flavus* on the fourth day. B. TLC results of AFB<sub>1</sub> produced by seven-day-old colonies after MSX treatment. SD is a standard AFB<sub>1</sub>. C. Quantification results of AFB<sub>1</sub> production after MSX treatment. Bars represent standard deviation from three independent experiments with three replicates each, and NS denotes no significant differences at  $P > 0.05$  as determined by Student's *t*-test.

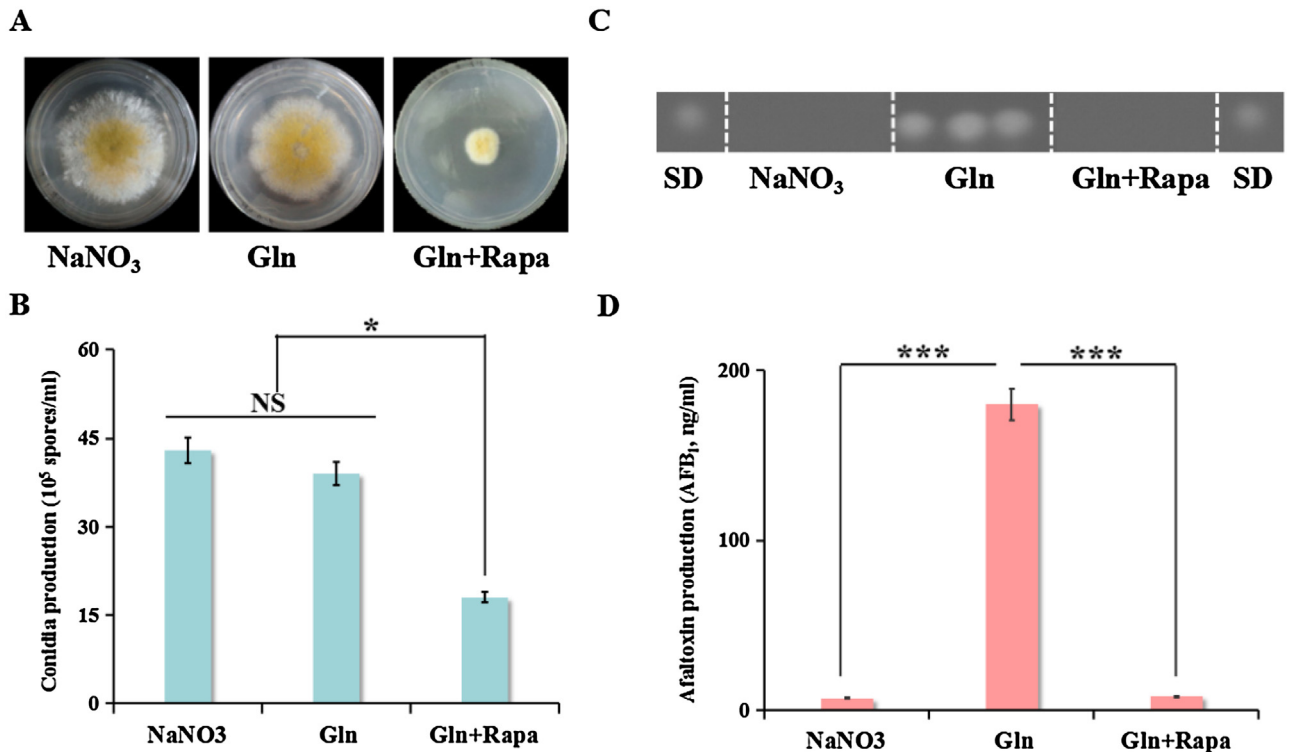


**Fig. 4.** The impacts of rapamycin treatment on growth, conidia and AFs biosynthesis of *A. flavus*. A. Morphological characterization of five-day *A. flavus* strains cultured on CD medium with indicated material at 28 °C in the dark. Rapamycin concentration is 200 ng/mL. B. Conidia amount of five-day *A. flavus* strains as in panel A. \*Significant at  $P < 0.05$  and NS denotes no significant differences at  $P > 0.05$  as determined by Student's *t*-test. C. AFB<sub>1</sub> results of *A. flavus* cultured as in panel A was detected by TLC. SD for standard AFB<sub>1</sub>. D. Analysis of AFB<sub>1</sub> production by *A. flavus* as in panel C. Bars represent standard deviation from three independent experiments with three replicates each. \*\*\*Significant at  $P < 0.001$  as determined by Student's *t*-test.

18 million of 151 bp paired-end reads were generated for each RNA-seq library. The reads from RNA-seq were aligned to *A. flavus* genome. An aggregate of 9995 expressed genes (FPKM > 0) in at least 3 samples were selected for subsequent DEGs analysis. The

sample homogeneity of the three control groups, with three replications, were analyzed. The samples were highly reproducible, and the experimental results were reliable and credible (Fig. 5A). The expression levels of nine cDNA libraries were delineated by

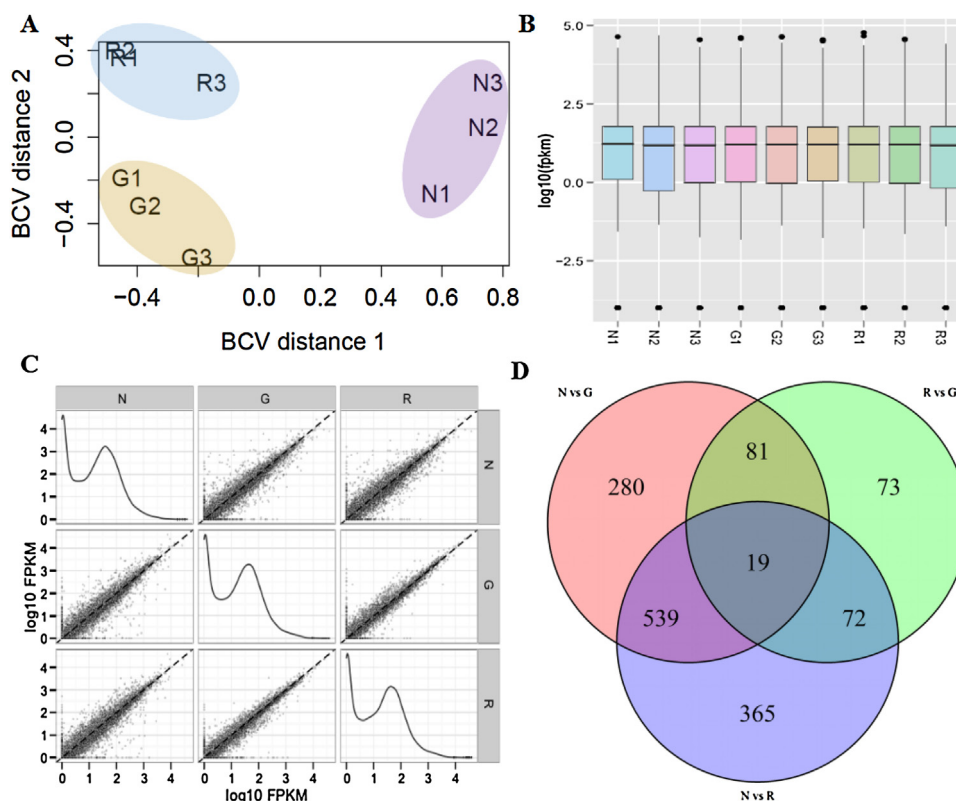


**Fig. 5.** The overall expression level of three parallel plates with three replications (NaNO<sub>3</sub> marked as N, Gln as G, and Gln plus rapamycin as R). A. The BCV (Biological Coefficient of Variation) distance of three parallel plates with three replications (1–3 stand for repeat number of each sample). B. The boxplot of overall expression level of three parallel plates with three replications. C. Pairwise comparison of whole gene expression level of three parallel plates. D. Venn diagram showing the overlap in N vs G, R vs G, and N vs R.

boxplot profiles (Fig. 5B), and a pairwise comparison of gene expression levels on three parallel plates was shown as Fig. 5C. The gene expression levels of the three samples were highly similar, indicating that the RNA-seq data were reliable. Gene differential expression analysis identified 919 DEGs ( $|\text{Fold change}| > 1$ , False discovery rate  $\leq 0.05$ ) between N and G, 245 DEGs between R and G, and 995 DEGs between N and R (Fig. 5D). In total, 1429 DEGs from the three pairwise comparisons.

### 3.6. Functional analysis and classifications of DEGs

To further study the transcriptome data of DEGs, GO was adopted to analyze all of the DEG functional classifications. The GO analysis showed that genes were down-regulated in G compared with in N and could be categorized into 13 functional classifications. The up-regulated genes in G compared with in N contained two functional classifications. There were 18 functional groups in the genes down-regulated in R compared with in N, six functional groups of up-regulated genes in R compared with in N, and seven functional groups of up-regulated genes in G compared with in R (Fig. 6). Most functional groups existed on either N or R, indicating that there was a larger difference between them. Furthermore, the significantly higher transcription levels of genes in N over those in G were involved in transporter activities, including the transmembrane transporter activity of amine, substrate-specific organic acids, amino acids and carboxylic acid, as well as oxidoreductase activities. However, the transcription levels of genes implicated in catalytic activity, monooxygenase activity, iron ion binding, heme binding, and tetrapyrrole binding were much higher in G than those in N and R. These results indicated that these genes might play important roles in regulating AF biosynthesis.

The KEGG Pathway Database was initiated to identify the biological pathways of DEGs, and these DEGs were found to be enriched in the 32 KEGG pathways. Among the 32 KEGG pathways, the most represented were those related to nitrogen metabolism, carbon metabolism, glycine, threonine, aspartate and glutamate metabolism, SMs biosynthesis, alpha-linolenic acid metabolism, and AF biosynthesis (Fig. 7). Moreover, several known regulatory factors participated in the nitrogen source-mediated regulation of secondary metabolite biosynthesis in fungi, which included the TOR protein kinase, GATA transcription factors AreA and AreB, nitrogen metabolite repression regulator NmrA, bZIP transcription factor MeaB, GS, ammonium permease MepB (the homolog MepA in *A. flavus*) and velvet protein Velf/VeA [30]. The transcriptome data showed that some of regulatory factors presented differential expression levels under the three culture conditions (Table S2), which suggested that these regulatory factors were likely to play critical roles in regulating nitrogen source metabolism and AF biosynthesis processes. These results revealed the extensive and complex relationships among nitrogen source metabolic pathways, the TOR signaling pathway and AF biosynthesis in *A. flavus*.

### 3.7. DEGs analysis associated with AF biosynthesis in *A. flavus*

To assess the regulation of AF biosynthesis under the three culture conditions, the expression levels of AF biosynthesis-associated genes were analyzed. In total, 24 DEGs relating to AF biosynthesis were identified. These genes were more highly expressed in G, which had the highest AF production (Fig. 1C and D). There were 21 DEGs shown in Fig. 8, and the other three DEGs were *aflA* (AFLA.139240), *aflMa* (AFLA.139290) and *aflCa* (AFLA.139400). The expression levels of *aflD*, *aflL*, *aflM*, *aflV* and *aflW* were reported to play significant roles in AF biosynthesis, and the expression levels of

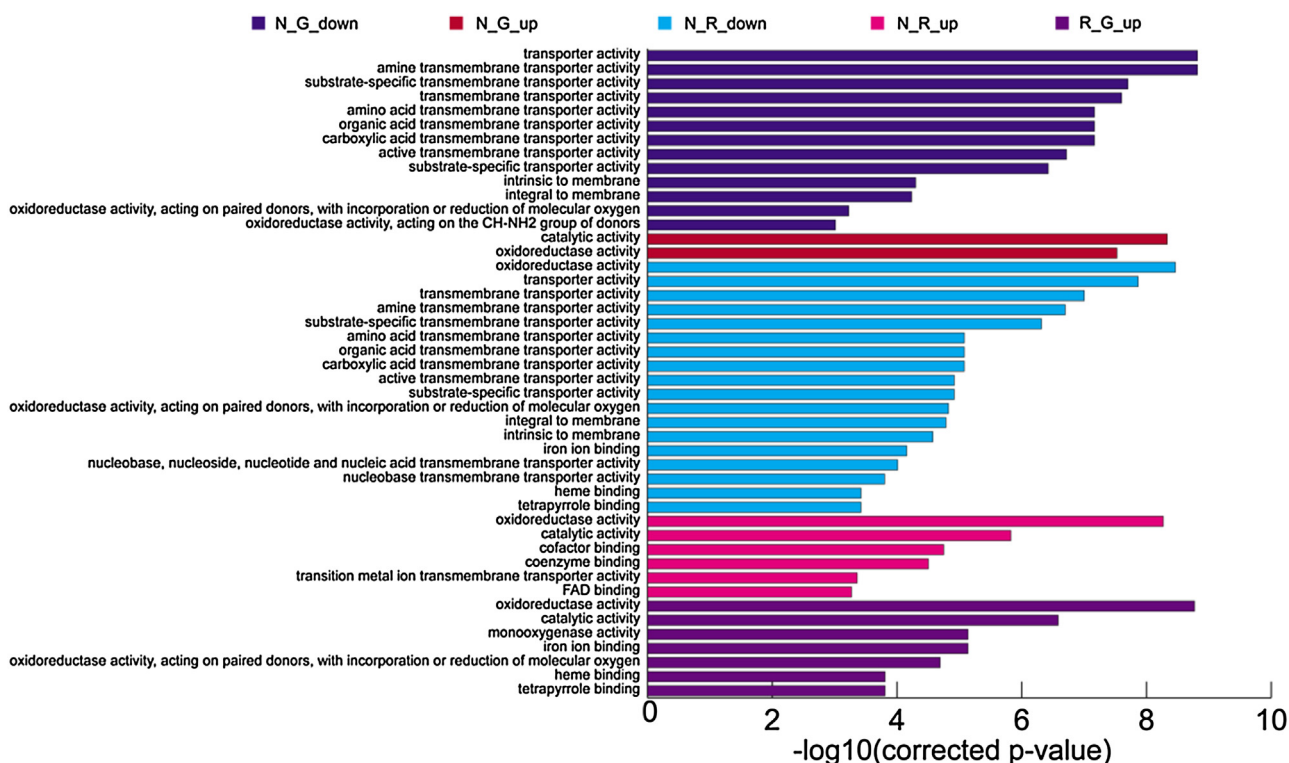


Fig. 6. GO enrichment analysis of DEGs in each treatment group.

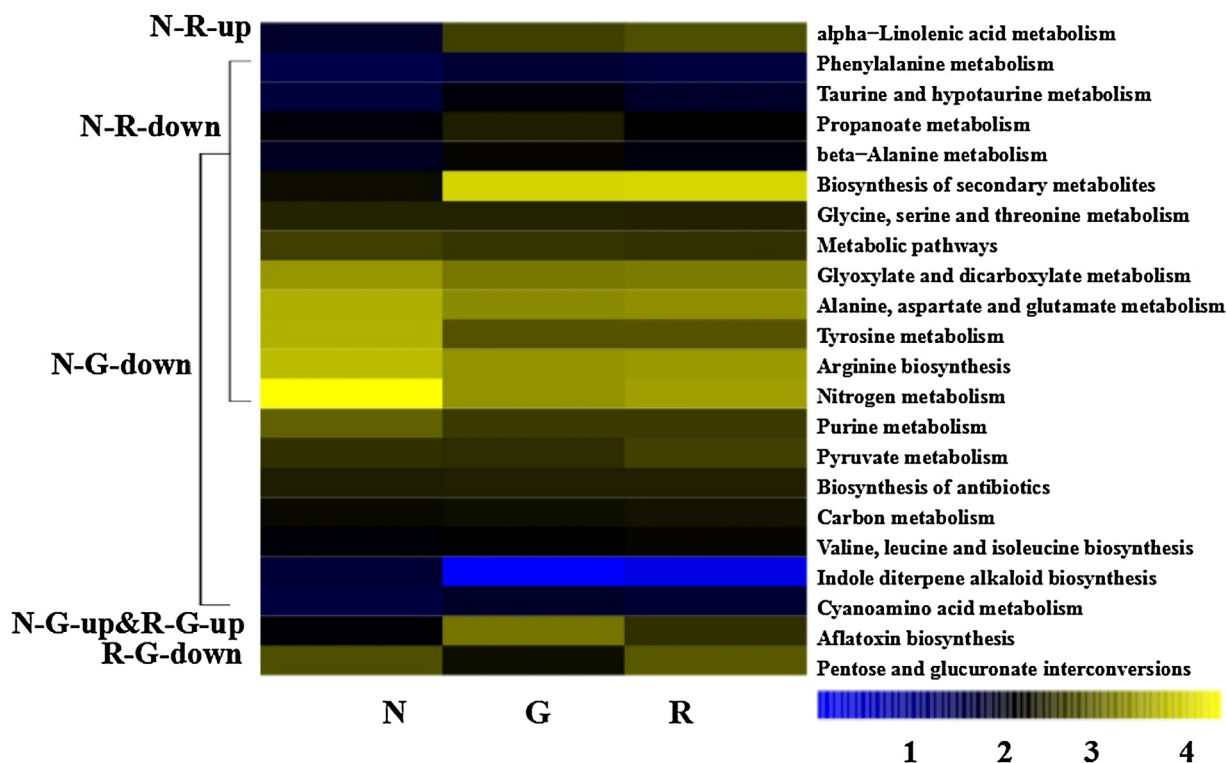
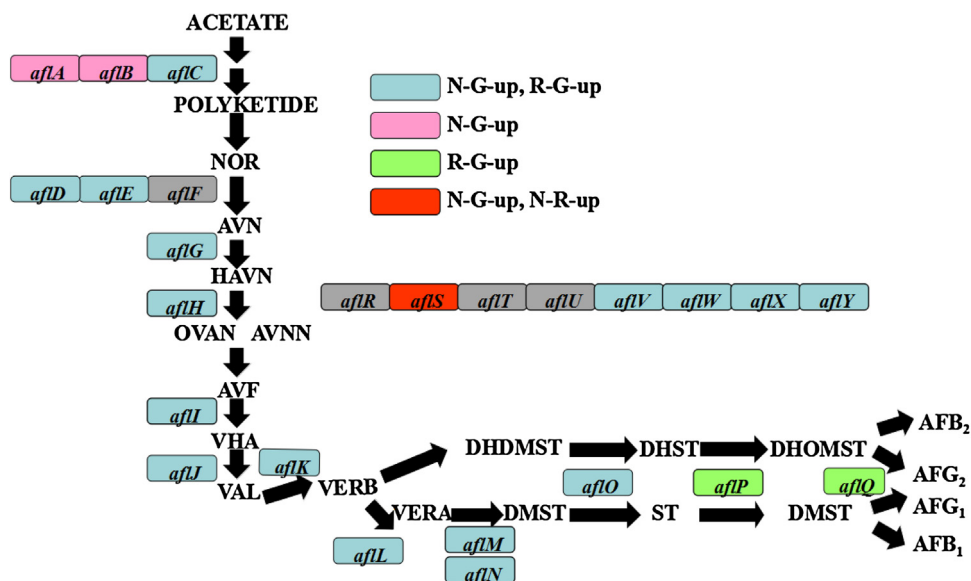


Fig. 7. KEGG analysis of DEGs. The heatmap showed 22 of 32 annotated pathways of DEGs among N, G and R. Different colors represented different expression levels of a particular metabolism pathway during the three groups. The numbers represented fold changes from low to high. Each row represented differentially expressed metabolism pathway. The data used to construct this heatmap was based on the  $\log_2$  value of the FPKM values of all DEGs in N, G and R.

these proteins affected AF production directly [5], which was consistent with the results of the study. Moreover, the expression levels of dehydrogenase (*aflH* and *aflE*), oxidase (*aflX*, *aflL* and *aflV*), cyclase (*aflA*, *aflB* and *aflC*), methyltransferase (*aflO* and *aflP*) and oxidore-

ductase (*aflQ* and *aflI*) were also quite important in AF formation, and their activities greatly influenced AF production. In addition, *aflR* was the most important regulatory gene in the AF biosynthesis gene cluster, and the expression change of *aflR* could cause the



**Fig. 8.** DEGs of AFs synthetic pathways determined by KEGG enrichment analysis. Genes in colored diamonds except for gray represented differentially expressed in N, G and R.

changes in other AF biosynthesis pathway genes. Additionally, *aflS* might be a regulatory gene controlling AF biosynthesis. Surprisingly, the transcript level of *aflR* did not obviously change under the three culture conditions, which might be related with the fact that the *aflR* expression level could be affected by various factors from environmental stimuli and nutritional conditions. However, a transcriptome analysis showed that the expression level of *aflS* was up-regulated in G compared with those in N and R, demonstrating the regulatory function of *aflS*. The results suggested that the Gln metabolism and TOR signaling pathway had regulatory effects on AF production in *A. flavus*.

### 3.8. qRT-PCR assays of the DEGs

To validate the expression data obtained by RNA-seq, qRT-PCR assays were performed for six protein coding genes, including two AF pathway genes, *aflO* and *aflQ*, two conidiation transcription factors, *abaA* and *brlA*, and two nitrogen metabolism-related genes, *niiA* and *niaD*. Based on the fold-changes of the six genes examined, the two methods were in general agreement and qualitatively similar, confirming the high reproducibility of the data (Fig. 9). Additionally, *niiA* and *niaD* had significantly higher expression levels in the N culture than in G or R, which was consistent with their functions in nitrate utilization. Moreover, the expression levels of the conidiation transcriptional genes and AF biosynthesis genes were down-regulated in R, which corroborated the rapamycin treatment's inhibition of AF and conidial production in *A. flavus* (Fig. 4).

## 4. Discussion

This study was initiated to explore possible crosstalk between the nitrogen response pathway and TOR cascade in relation to AF production in *A. flavus*. First, our experiments showed that the nitrogen sources of ammonium and some amino acids promoted AF production, and that nitrate had suppressive effects on AF biosynthesis, suggesting that the nitrogen metabolism pathways played important regulatory roles in AF formation. In addition, there were nitrogen sources-specific effects on AF biosynthesis. However, how fungi could sense different nitrogen sources is not clearly understood. Nitrogen sources with identical ammonium

ions but different negative ions (for instance,  $\text{NH}_4\text{Cl}$ ,  $(\text{NH}_4)_2\text{SO}_4$  and  $\text{NH}_4\text{NO}_3$ ) had varied effects on growth and AF production. These results indicated that distinct ions might affect AF biosynthesis, and also revealed the complexity and subtlety of the nitrogen source's effects on the regulation of AF biosynthesis in *A. flavus*.

Gln induced the maximal AFB<sub>1</sub> production in *A. flavus*. However, the effects of Gln concentrations on AF biosynthesis revealed a threshold for AFB<sub>1</sub> production. Interestingly, the threshold effect was just for AFB<sub>1</sub> production not for AFB<sub>2</sub> (data not shown). Unexpectedly, the MSX treatment showed little impact on AF production, but the hyphae yielded fluffy cotton-like colonies after MSX treatment, which was likely associated with mutations in *fluG*, consisting of a C-terminal GS domain, which was postulated to synthesize a diffusible factor that initiates conidiation [41]. Additionally, for *A. flavus*, the deletion of *fluG* did not affect AF production [42]. This suggested that there were different AF biosynthesis and growth responses to MSX. However, the specific molecular regulatory mechanisms of AF biosynthesis and growth are still unclear and need to be further explored. Additionally, a rapamycin treatment restrained growth, and conidial and AF production in *A. flavus*, revealing that the TOR signaling pathway was very important in the regulation of the nitrogen response pathway and AF biosynthesis.

The transcriptome data demonstrated certain correlations among the nitrogen source signaling pathway, TOR kinase and AF biosynthesis pathway. In particular, some genes in the AF biosynthesis gene cluster were up-regulated in G compared with in N and R, which accounted for Gln promoting AF biosynthesis. Moreover, a wide variety of genes associated with nitrogen metabolism and AF biosynthesis showed differential expression levels after the rapamycin treatment, which suggested that the TOR signaling pathway could regulate nitrogen metabolism and AF biosynthesis [40]. The transcriptome analysis also showed that the genes of the nitrogen metabolism and TOR cascade pathways might be diverse but overlap in the regulation of AF biosynthesis, indicating possible interactions between the nitrogen source metabolism and TOR cascade pathways in controlling AF biosynthesis. This was the first time that the nitrogen response and TOR signaling pathways were linked with AF biosynthesis in *A. flavus*, although the AF biosynthesis process and a clustered pathway of genes associated with AF biosynthesis had been known for more than a decade [10].

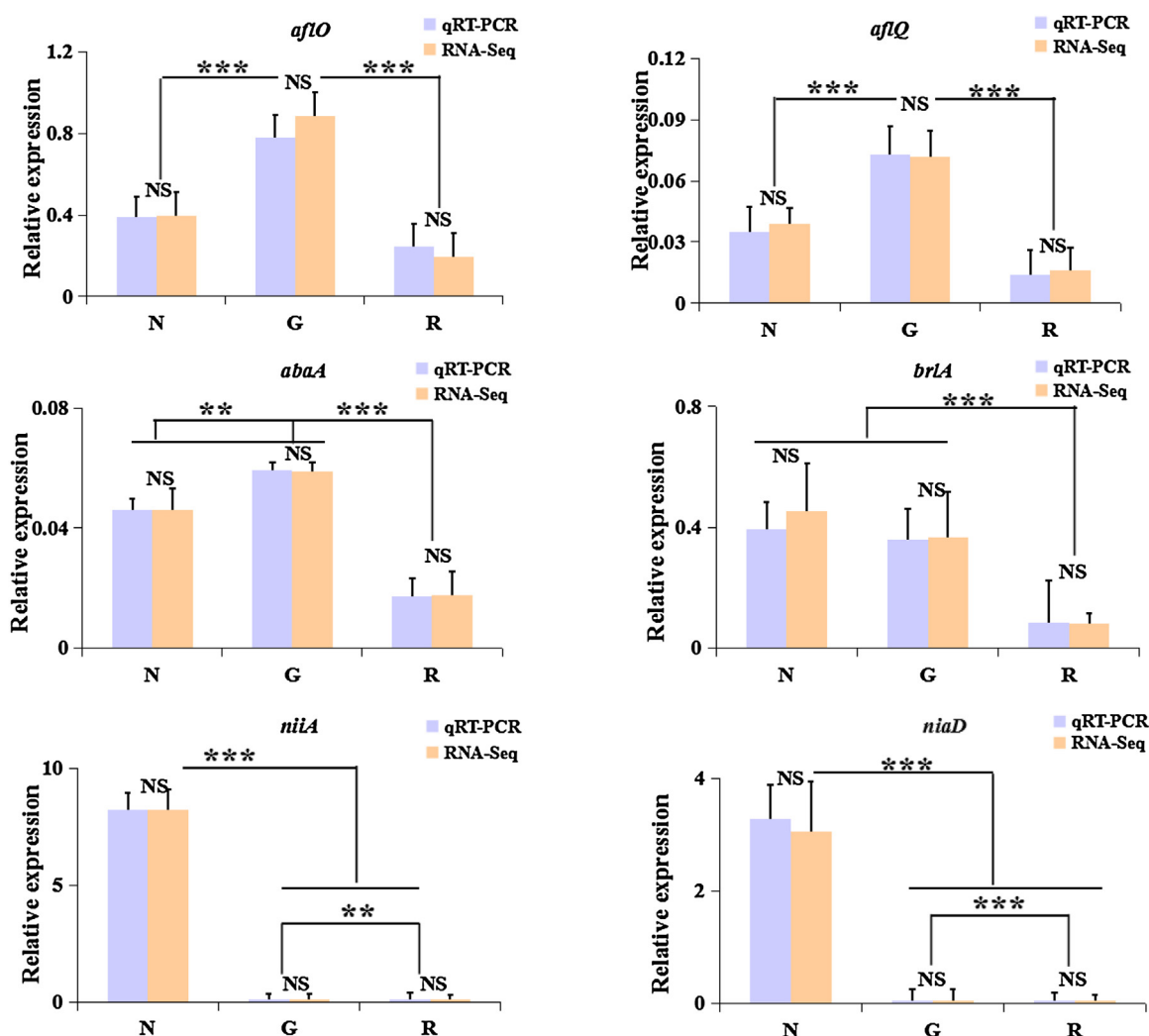


**Fig. 9.** QRT-PCR results of differentially expressed genes (NaNO<sub>3</sub> marked as N, Gln as G, and Gln plus rapamycin as R). The relative expression level of each gene was expressed as the fold change of N, G and R in the RNA-Seq data (orange bar) and qRT-PCR data (royal purple bar). The *A. flavus*  $\beta$ -tubulin gene was used as an internal control to normalize the expression data. The bars represent the standard deviation from three independent experiments with three replicates each.

Thus, this work contributes to a general understanding of the nitrogen regulation of AF biosynthesis in *A. flavus*. Additionally, our results provided an opportunity to better understand the molecular basis of the nitrogen regulatory network, as well as AF biosynthesis and the TOR signaling pathway. By analyzing transcriptome data, new insights were gained into how nitrogen sources regulate the morphology of, and SMs biosynthesis in, *A. flavus*, which are essential to facilitate the development of efficient control strategies against AFs.

#### Author contributions

Conceived and designed the experiments: BW, XH and Shihua W. Performed the experiments: XH and MQ. Analyzed the data: XH, YB, ZL and Sen W. Contributed reagents/materials/analysis tools: XN, FZ, ZZ and JY. Wrote the paper: BW, XH, YB and ZL. Support financially and administratively, final approval of manuscript: Shihua W.

#### Competing financial interests

The authors declare no competing financial interests.

#### Acknowledgments

We thank Prof. Zhumei He (Sun Yat-sen University, Guangzhou, China) for supplying *Aspergillus flavus* strain NRRL3357. This research was supported by the National 973 Program from the Ministry of Science and Technology of China (2013CB127802), the National Natural Science Foundation of China (31172297, 31000961 and 31400100), and The Key Project of Science and Technology in Fujian Province (2014Y0047).

#### Appendix A. Supplementary data

Supplementary data associated with this article can be found, in the online version, at <http://dx.doi.org/10.1016/j.jhazmat.2016.11.043>.

#### References

- [1] P.J. Cotty, Virulence and cultural characteristics of two *Aspergillus flavus* strains pathogenic on cotton, *Phytopathology* 79 (1989) 808–814.
- [2] D.M. Geiser, W.E. Timberlake, M.L. Arnold, Loss of meiosis in *Aspergillus*, *Mol. Biol. Evol.* 13 (1996) 809–817.
- [3] M.A. Klich, *Aspergillus flavus*: the major producer of aflatoxin, *Mol. Plant Pathol.* 8 (2007) 713–722.

- [4] T. Michailides, T. Thomidis, First report of *Aspergillus flavus* causing fruit rots of peaches in Greece, *Plant Pathol.* 56 (2007) 352.
- [5] J. Yu, Current understanding on aflatoxin biosynthesis and future perspective in reducing aflatoxin contamination, *Toxins* 4 (2012) 1024–1057.
- [6] G.A. Payne, M.P. Brown, Genetics and physiology of aflatoxin biosynthesis, *Annu. Rev. Phytopathol.* 36 (1998) 329–362.
- [7] M. Hedayati, A.C. Pasqualotto, P.A. Warn, et al., *Aspergillus flavus*: human pathogen, allergen and mycotoxin producer, *Microbiology* 153 (2007) 1677–1692.
- [8] Y.H. Bai, F.X. Lan, W.Q. Yang, et al., sRNA profiling in *Aspergillus flavus* reveals differentially expressed miRNA-like RNAs response to water activity and temperature, *Fungal Genet. Biol.* 3 (2015) 1–7.
- [9] T.E. Cleveland, J. Yu, N. Fedorova, Potential of *Aspergillus flavus* genomics for applications in biotechnology, *Trends Biotechnol.* 27 (2009) 151–157.
- [10] J. Yu, C. Perng-Kuang, K.C. Ehrlich, Clustered pathway genes in aflatoxin biosynthesis, *Appl. Environ. Microbiol.* 70 (2004) 1253–1262.
- [11] S. Amaike, K.J. Affeldt, W.B. Yin, et al., The bZIP protein MeaB mediates virulence attributes in *Aspergillus flavus*, *PLoS One* 8 (2013) e74030.
- [12] F. Zhang, H. Zhong, X.Y. Han, Proteomic profile of *Aspergillus flavus* in response to water activity, *Fungal Biol.* 119 (2015) 114–124.
- [13] J.W. Bennett, K.E. Papa, The aflatoxigenic *Aspergillus* spp., *Adv. Plant Pathol.* 6 (1988) 265–279.
- [14] K. Yabe, H. Nakamura, Y. Ando, Isolation and characterization of *Aspergillus parasiticus* mutants with impaired aflatoxin production by a novel tip culture method, *Appl. Environ. Microbiol.* 54 (1988) 2096–2100.
- [15] S.P. Kale, J.W. Cary, D. Bhatnagar, J.W. Bennett, Characterization of experimentally induced, nonaflatoxigenic variant strains of *Aspergillus parasiticus*, *Appl. Environ. Microbiol.* 62 (1996) 3399–3404.
- [16] K.H. Wong, M.J. Hynes, M.A. Davis, Recent advances in nitrogen regulation: a comparison between *Saccharomyces cerevisiae* and filamentous fungi, *Eukaryot. Cell* 7 (2008) 917–925.
- [17] G.A. Marzluf, Genetic regulation of nitrogen metabolism in the fungi, *Microbiol. Mol. Biol. Rev.* 61 (1997) 17–32.
- [18] N.D. Davis, U.L. Diener, V.P. Agnihotri, Production of aflatoxins B<sub>1</sub> and G<sub>1</sub> in chemically defined medium, *Mycopathol. Mycol. Appl.* 31 (1967) 251–256.
- [19] T.V. Reddy, L. Viswanathan, T.A. Venkatasubramanian, Factors affecting aflatoxin production by *Aspergillus parasiticus* in a chemically defined medium, *J. Gen. Microbiol.* 114 (1979) 409–413.
- [20] P.K. Chang, J. Yu, D. Bhatnagar, Characterization of the *Aspergillus parasiticus* major nitrogen regulatory gene, *areA*, *Biochim. Biophys. Acta* 1491 (2000) 263–266.
- [21] W. Du, G.R. Obrian, G.A. Payne, Function and regulation of *afll* in the accumulation of aflatoxin early pathway intermediate in *Aspergillus flavus*, *J. Food Addit. Contam.* 24 (2007) 1043–1050.
- [22] A.M. Calvo, J.W. Bok, W. Brooks, VeA is required for toxin and sclerotial production in *Aspergillus parasiticus*, *Appl. Environ. Microbiol.* 70 (2004) 4733–4739.
- [23] M.S. López-Berges, N. Rispall, R.C. Prados-Rosales, A nitrogen response pathway regulates virulence functions in *Fusarium oxysporum* via the protein kinase TOR and the bZIP protein MeaB, *Plant Cell* 22 (2010) 2459–2475.
- [24] N.C. Barbet, U. Schneider, S.B. Helliwell, TOR controls translation initiation and early G1 progression in yeast, *Mol. Biol. Cell* 7 (1996) 25–42.
- [25] T. Beck, M.N. Hall, The TOR signalling pathway controls nuclear localization of nutrient-regulated transcription factors, *Nature* 402 (1999) 689–692.
- [26] J.L. Crespo, M.N. Hall, Elucidating TOR signaling and rapamycin action: lessons from *Saccharomyces cerevisiae*, *Microbiol. Mol. Biol. Rev.* 66 (2002) 579–591.
- [27] R.B. Todd, J.A. Fraser, K.H. Wong, et al., Nuclear accumulation of the GATA factor AreA in response to complete nitrogen starvation by regulation of nuclear export, *Eukaryot. Cell* 4 (2005) 1646–1653.
- [28] K. Min, Y. Shin, H. Son, Functional analyses of the nitrogen regulatory gene *areA* in *Gibberella zeae*, *FEMS Microbiol. Lett.* 334 (2012) 66–73.
- [29] C.C. Hunter, K.S. Siebert, D.J. Downes, Multiple nuclear localization signals mediate nuclear localization of the GATA transcription factor AreA, *Eukaryot. Cell* 13 (2014) 527–538.
- [30] B. Tudzynski, Nitrogen regulation of fungal secondary metabolism in Fungi, *Front. Microbiol.* 5 (2014) 1–15.
- [31] G.J. Fitzgibbon, I.Y. Morozov, M.G. Jones, Genetic analysis of the TOR Pathway in *Aspergillus nidulans*, *Eukaryot. Cell* 4 (2005) 1595–1598.
- [32] S. Teichert, M. Wottawa, B. Schönig, Role of the *Fusarium fujikuroi* TOR kinase in nitrogen regulation and secondary metabolism, *Eukaryot. Cell* 5 (2006) 1807–1819.
- [33] K. Twumasi-Boateng, Y. Yan, C. Dan, Transcriptional profiling identifies a role for *BrlA* in the response to nitrogen depletion and for *StuA* in the regulation of secondary metabolite clusters in *Aspergillus fumigatus*, *Eukaryot. Cell* 8 (2009) 104–115.
- [34] M. Ofitserova, S. Nerkar, M. Pickering, multiresidue mycotoxin analysis in corn grain by column high-performance liquid chromatography with post-column photochemical and chemical derivatization: single-laboratory validation, *J. AOAC Int.* 92 (2009) 15–25.
- [35] C. Trapnell, A. Roberts, L. Goff, Differential gene and transcript expression analysis of RNA-seq experiments with TopHat and Cufflinks, *Nat. Protoc.* 7 (3) (2012) 562–578.
- [36] L. Wang, Z. Feng, X. Wang, DEGseq: an R package for identifying differentially expressed genes from RNA-seq data, *Bioinformatics* 26 (2010) 136–138.
- [37] M.E. Smoot, K. Ono, J. Ruscheinski, et al., Cytoscape 2.8: new features for data integration and network visualization, *Bioinformatics* 27 (3) (2011) 431–432.
- [38] K.J. Livak, T.D. Schmittgen, Analysis of relative gene expression data using real-time quantitative PCR and the 2(-Delta C(T)) Method, *Methods* 25 (2001) 402–408.
- [39] J. Fernandez, J.D. Wright, D. Hartline, et al., Principles of carbon catabolite repression in the rice blast fungus: *tps1*, *Nmr1-3*, and a MATE-family pump regulate glucose metabolism during infection, *PLoS Genet.* 8 (5) (2012) e1002673.
- [40] R. Loewith, M.N. Hall, Target of rapamycin (TOR) in nutrient signaling and growth control, *Genetics* 189 (4) (2011) 1177–1201.
- [41] B.N. Lee, T.H. Adams, The *Aspergillus nidulans fluG* gene is required for production of an extracellular developmental signal and is related to prokaryotic glutamine synthetase I, *Genes Dev.* 8 (1994) 641–651.
- [42] P.K. Chang, L.L. Scharfenstein, B. Mack, Deletion of the *Aspergillus flavus* orthologue of *Aspergillus nidulans fluG* reduces conidiation, promotes sclerotial production, but does not abolish aflatoxin biosynthesis, *Appl. Environ. Microbiol.* 78 (2012) 7557–7563.